Formulation of Transport in a Catchment-Scale Conceptual Model

by

Lotte de Vos

to obtain the degree of Master of Science
at the Delft University of Technology,
to be defended publicly on Monday October 23, 2017 at 14:30 AM.

Student number:	1528653	
Thesis committee:	Dr. M. Hrachowitz,	TU Delft, Water Resource Management
	Prof. dr. ir. H.H.G. Savenije,	TU Delft, Water Resource Management
	Dr. B.M. van Breukelen,	TU Delft, Sanitary Engineering

TU Delft

Acknowledgements

Firstly,I would like to thank Markus Hrachowitz for his guidance and helping me whenever I had questions. I am also grateful to Prof. Huub Savenije for his supervision, and for his inspiring classes in hydrology. Thank you also to Boris van Breukelen for being in my committee.

A special thanks to my parents, for just always being there and putting everything in perspective. To my sister, for being the sweetest person there is, and to my brothers. If I have any talent for scientific thinking it is probably because you always made me defend everything I say ;)

Thanks to Lottie, for bringing wine when I needed it ;) Lastly, I would like to thank my amazing roommates. Charlie, thanks for your mental support during my thesis but also before. Katharina, thank you for being there until the very last minute! Nadieh, matlab-hero and buddy for life, thanks for making any situation a funny situation.

Lotte de Vos
Delft, 17th October, 2017

Abstract

Standard conceptual hydrological models can rarely accommodate stream tracer dynamics at the catchment scale. They rely on the generation of runoff through the propagation of a pressure wave and do not account for the actual advective movement of particles. Over the last years different model frameworks have been developed to account for this shortcoming. The difference between the frameworks lies in whether they are based on mixing coefficients or storage age selection functions. Both methods have shown their ability to capture the stream chemistry response. It is however not clear how these distinct approaches compare to each other and to reality.

To provide more clarification in this matter, this research applied both frameworks separately to model the hydrological and stream water chemistry response for a specific catchment. The results are analysed using the concept of transit times, where information on the fluxes and states in all model components is used to generate distributions that describe the age structure of water. By comparing the distributions generated by both methods and by evaluating the overall model performances, more insight is gained on the two frameworks and on their ability to capture subsurface mixing dynamics.

From the results of this research it is concluded that both frameworks show similar performance. They are however conceptually different, which might have implications for their ability to capture specific dynamics. These implications depend on the characteristics of the catchment of interest. It is still concluded however that performance for each frameworks is likely to be similar. Because the model description of the Mixing Coefficient framework is less complex, it is recommended to continue research with this framework.

A visitor to Picasso's studio found the artist gazing disconsolately at a painting on the easel.

"It's a masterpiece," said the visitor, hoping to cheer him up.

"No, the nose is all wrong," Picasso said. "It throws the whole picture out of perspective."

"Then why not alter the nose?"

"Impossible," replied Picasso. "I can't find it."

Contents

List of Figures

List of Tables

1 Introduction

1.1. Introduction

The effects of hydrological processes on societies and nature are widespread. Hydrological modelling is essential to quantify these effects. It can be used for the prediction of floods and droughts, and to determine the measures that need to be taken to prevent damage. By correctly describing the hydrological processes, models should be able to predict the behaviour of a hydrological system even when it is subject to changes in the environment.

A model however remains merely an interpretation of reality and is never a perfect representation. This is especially obvious in conceptual modelling, where scientists create models using their own perception of the dominant processes. While this type of modelling has great advantages in terms of computational efficiency and parsimoniousness, it can become difficult to assess the realism of the models. Even in cases where good results are generated, it is sometimes unclear whether these are obtained for the right reasons (Kirchner, 2006). As long as there's uncertainty in this matter, there's uncertainty in the predictive capacity of the model, especially when environmental circumstances change. Still, conceptual modelling is considered to be a very useful tool and over the last years progress has been made to create hydrological models that are closer to reality.

One of the challenges in catchment-scale conceptual models is that they rarely accommodate stream tracer dynamics. This is because these models usually rely on the generation of runoff through the propagation of a pressure wave, thereby not accounting for the actual advective movement of particles. When more information is needed about the qualitative response of a watershed, for instance in the area of pollution prediction and control, this is not sufficient. At the other side of the spectrum there are the water quality models, which address biogeochemical processes but usually employ overly simplistic descriptions of the hydrological processes (Hrachowitz et al., 2010). Because of this, they are unable to capture the effect of the hydrological processes on the biogeochemical behaviour (e.g., the effect of evaporation on solute concentrations). In order to accurately describe the stream chemistry response of a catchment, there is a need for models that better integrate these two worlds.

1.2. Connecting water quality and hydrology

In the past decades, several methods have been developed to account for the individual flow paths of particles at the catchment-scale. A commonly used metric in this effort is the time particles spend in catchments, also referred to as transit times. The transit time τ of a water particle is the time it takes for that particle to travel from the input boundary of the system (at time t_{in}) to the output boundary (at time t_{out}) (McDonnell et al., 2010):

$$\tau = t_{out} - t_{in} \tag{1.1}$$

The probability distribution of transit times reveals information about the flow pathways and the vulnerability of a catchment to pollution spreading. As such, it is used as a fundamental average catchment property

(Van Der Velde et al., 2012).

In the past, different models have been developed that evolve around the concept of transit times. Traditional models often rely on a convolution integral approach (McGuire and McDonnell, 2006), in which transit times are estimated by analyzing input-output relationships for conservative tracers. This approach originates from theory provided in contributions by Maloszewski Zuber (1982,1993), who model the routing of water with a mathematical expression of a transit time distribution (TTD):

$$c_{out}(t) = \int_0^\infty g(\tau) c_{in}(t-\tau) d\tau \tag{1.2}$$

where τ is the transit time and t is the time of exit from the system, so that $(t-\tau)$ represents the time of entry into the system. The output tracer concentration $c_{out}(t)$ is then equal to the combined tracer input concentrations from any entrance time $(t-\tau)$ in the past, weighed by the transfer function $g(\tau)$. This transfer function represents an assumed time-invariant, lumped TTD of tracers in the catchment. While this assumption might hold for groundwater systems nearing steady state conditions, it is not realistic for other situations (Zuber, 1986).

Results of studies following the convolution integral approach have nevertheless been useful to generate more understanding of catchment-scale transport processes. For example, several studies have indicated a relation between landscape organization and derived TTDs (McGlynn et al., 2003; McGuire et al., 2005; Hrachowitz et al., 2010). Hrachowitz et al. (2009b) and Tetzlaff et al. (2011) concluded that soil type, topography and climatic conditions have strong control over mean travel times, especially in systems that are dominated by surface waters. For larger sized catchments, Speed et al. (2010) also found a relation between soil type and transit time, although the variation was less. Roa-García and Weiler (2010) showed that these relations can be useful to assess the effect of land use change, by showing the different effects of forest cover and grassland in similar catchments. This study also revealed a significant influence of antecedent wetness conditions.

The above mentioned relations are usually time-variant and thus emphasize the time variability of catchment-scale transport processes. In the last decade, more studies have suggested that TTDs should reflect this variability (e.g., Botter, 2012; Van Der Velde et al., 2010; McDonnell et al., 2010; Hrachowitz et al., 2009a; Roa-García and Weiler, 2010). Selection of a TTD that can be matched with functional catchment behaviour therefore is a big challenge (McGuire and McDonnell, 2006). An alternative modeling approach that avoids some of the complications of TTD selection is the use of conceptual hydrological models that are coupled with mixing volumes in their storage components (Hrachowitz et al., 2016). Instead of selecting a TTD, the focus is on choosing the right expression for mixing. This expression then influences the way outflows are composed of water volumes of different ages, which is represented by the shape of TTDs.

Shifting the focus to subsurface mixing is supported by previous research that has suggested that this mixing controls *how* the weather variability and climate affect the variability of TTDs (Botter et al., 2011; Soulsby et al., 2009). Several studies have also highlighted the potential effect of different degrees of subsurface mixing on generated transit time distributions (Kirchner et al., 2000; Godsey et al., 2010; Fenicia et al., 2010; Hrachowitz et al., 2013). Catchment-scale mixing processes however cannot be quantified directly, and there is still great uncertainty surrounding the choice of mixing assumptions (Hrachowitz et al., 2016).

1.3. Research objective

In recent studies, two different frameworks have been developed that include subsurface mixing in a conceptual hydrological model. The difference between the two frameworks lies in whether the desired effect is achieved by applying mixing coefficients or through storage age selection functions. Both frameworks have shown their potential to capture the stream chemistry response. Up until this research, it has been unclear how the two approaches would compare to each other when evaluated more closely. The aim of this research was to provide clarification on this matter. Building on the notion that models are useful tools to test hypothesis concerning the catchment-scale transport processes (Benettin et al., 2015a), this research performs a comparative study in which the effects of two frameworks are evaluated. The objective of this study was thus to investigate the effect of the different mixing assumptions on the generated Transit Time Distributions. Through this analysis, an assessment is made of their realism which ultimately contributes to the

development of integrated catchment-scale models that account for both the qualitative and the quantitative response.

1.4. Outline report

In the next chapters, more theory will be presented on conceptual, integrated catchment-scale models. An elaboration will be given on the processes behind catchment-scale, subsurface mixing, after which the two developed frameworks will be introduced. This will be followed by an explanation of the methodology, after which the results will be presented. The report ends with a discussion on the results and recommendations for future research.

2
Background

2.1. Hydrology at the catchment-scale

Hydrology can be studied at different spatial scales. In general, catchments are recognized as suitable landscape units for hydrological studies. The defined boundaries of a catchment enable hydrologists to study all integrated aspects of the hydrological cycle, including the cycling of sediments and dissolved constituents (Sivapalan, 2005; Wagener et al., 2004). However, within the field of catchment-scale hydrological models, there are different approaches. These approaches can be roughly divided in two subgroups: physically based models and conceptual models. The frameworks studied in this research belong to the realm of conceptual models. In order to provide some understanding on why one would choose the conceptual approach when trying to model stream tracer dynamics, both methods will be shortly explained and discussed. Hereafter, the focus of the research will be entirely on conceptual modelling.

2.1.1. Physically based models

Physically based models attempt to capture the governing dynamics by explicitly accounting for as many processes as possible (Hrachowitz and Clark, 2017). In order to do so, they usually rely on detailed descriptions of the flow and transport processes. Ideally, these models can completely rely on direct observations without parameter calibration. At the catchment scale however the spatial heterogeneity of both the system forcings and its boundary conditions cannot be sufficiently described with observations (Hrachowitz et al., 2016). This lack of information, in combination with the fact that there is always some degree of conceptualization at the level of the smallest grid cell, fosters the need for parameter calibration. This, together with the detailed level of description, causes these models to be computationally highly demanding.

The high computational costs however do not guarantee more reliable results. Instead of small-scale behaviour being accurately extrapolated into an overall system response, it is more likely that the many paramaters that are needed start compensating for each other. These models have indeed shown to be highly susceptible to equifinality, which is when different combinations of parameter values result in equally good model performances. If this occurs, it is very difficult to assess which parameters represent reality best.

In short, these distributed, physically-based models are highly complex, computationally challenging and they do not necessarily lead to better knowledge of the catchment characteristics. While there has been progress to improve their ability to account for non-linear behaviour and spatial heterogeneity (Hrachowitz et al., 2016), the aforementioned difficulties still limit their application at the catchment-scale. It is for this reason that the hydrological community started shifting its attention towards conceptual models.

2.1.2. Conceptual models

Conceptual models are much simpler in their representation of the catchment. In conceptual modelling, hydrologists use their own perception of the most relevant processes to create models. These models consist of a combination of storage components that are linked through fluxes and can be customized based on perceived dominant processes. In their holistic approach, these models utilize the self-organizing behaviour

of catchments. This allows them to capture the dominant processes while remaining parsimonious. There are however also downsides to these models.
One of the challenges is that it can become difficult to relate a conceptual model to reality. The parameters are physical descriptions of reality at the scale of the model domain, thereby integrating spatial heterogeneity and domain-internal feedback processes (Hrachowitz and Clark, 2017). While they can be well related to reality (Fenicia et al., 2016), they can usually not be measured. Because of this, it is often uncertain whether the results are obtained for the right reasons. This is highly relevant when one wishes to use a conceptual model for prediction. There are ways to obtain more confidence in the results (e.g., model validation) but it is a difficult challenge to overcome.

Particularly interesting for this research is that conceptual models don't simulate single particle behaviour. Since the aim of a conceptual model is not to reproduce exactly what is occuring at the small scale but rather to capture patterns that are governing at the catchment-scale, the advective movement of particles is neglected. Instead, the main runoff processes are described in a manner that accounts for the propagation of a pressure wave. This is done by using the elevation head as the main driving force for transport, as is illustrated in Figure 2.1.

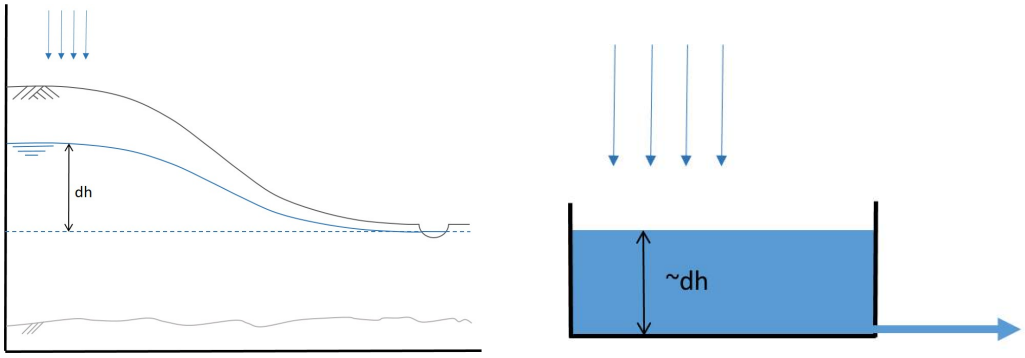

(a) catchment (b) bucket model

Figure 2.1: (a) schematization of a catchment and (b) the representation of the catchment by a conceptual bucket model.

While this conceptualization has shown to be able to generate the quantitative response (Fenicia et al., 2008), it lacks ability to capture the qualitative response. For this, the advective movement of particles should be taken into account. This is confirmed by several tracer studies that have found cases where rainfall inputs resulted in hydrological responses that led to limited fluctuations in stream water solute concentrations (Kirchner et al., 2000; Harman, 2015)

The delay in the stream chemistry response is mainly caused by dispersive mixing processes that influence the advective movements of particles (Hrachowitz et al., 2016). When more knowledge about the water quality conditions of a catchment is needed it is therefore necessary to account for this difference between the hydrological response and the stream chemistry response (or the difference between the wave *celerity* and the *velocity* of solutes). To this end, frameworks have been developed that include the effects of catchment-scale mixing in a conceptual model. In this research, the performance of these frameworks is evaluated. Before moving on to their details however, paragraph 2.2 will provide more background information of what catchment-scale mixing entails, to provide a better understanding of the dynamics that these frameworks are trying to capture.

2.2. Catchment-scale subsurface mixing

At the catchment-scale, mixing is largely a combination of two processes (Hrachowitz et al., 2016). Firstly, it accounts for the different effective flow velocities of particles that have entered the system at one particular location. For example, in Figure 2.2 a possible trajectory of a water particle is illustrated. Another particle that enters the catchment at the exact same time and location, will follow a different trajectory. This mixing process is largely a manifestation of the pore structure of the flow media (i.e., kinematic dispersion). The second process describes the in-stream mixing of water particles that enter the catchment at different times and locations, that are being routed to the stream through different flow routes. This is a manifestation of the distribution of flow path lengths (i.e., geomorphological dispersion). These mixing processes cause the water particles to flow along varying, individual trajectories. As depicted in Figure 2.2, a single particle could infiltrate in the soil and even reach the groundwater layer, causing a considerable delay in the time of arrival at the stream.

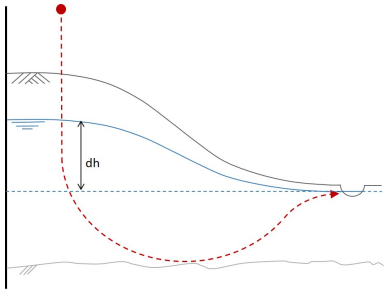

Figure 2.2: schematized particle trajectory in a catchment

The question of subsurface mixing however is of ongoing research. Next to these dispersive mixing processes, there are other dynamics that are of influence, for example the water uptake by vegetation. In an opinion article by McDonnell (2014) the hypothesis was posed that there are actually two water worlds in the subsurface, where transpiration by trees uses water from a different pool than the other hydrological processes (infiltration, groundwater recharge, hillslope runoff and streamflow). Studies like these emphasize that there is still uncertainty as to what is actually happening in the subsurface, with both physical and geochemical processes adding to its complexity (Ali et al., 2014). This uncertainty adds to the complexity of trying to capture these dynamics in a model. Still, progress has been made which has provided us with viable frameworks.

2.3. The effect of mixing on transit times distributions

The subsurface mixing processes cause the age distribution of water in the storage to be different than the age distribution of water in the outgoing fluxes. Because of this notion, it is relevant to make a distinction between the different types of travel time distributions. There are in fact three types that can be defined:

Forward TTD Distribution of time lags that a water volume that enters the system at a given point in time, t_i, will have experienced once it has been routed completely through the system

Backward TTD Distribution of water volumes of different ages, leaving the system at a given point in time t

Residence Time Distribution (RTD) Distribution of water volumes of different ages, stored in a system at a given point in time t

From the definition it follows that in forward tracking, a particle injection at a given time t_{in} is selected and the subsequent exit times are followed (Benettin et al., 2015b). In backward tracking on the other hand, the focus is on a volume of water that reaches the outlet at a given time t_{out}. The various entrance times of the particles within this volume are then tracked backwards in time. The forward and backward distributions are equal only when there are steady-state conditions (Zuber, 1986), which in reality is never the case. They are however interdependent, and can be related by continuity (Benettin et al., 2015b; Niemi, 1977). Because backward distributions reflect inputs and transport processes that occurred prior to the sampling time, they are more suitable for studying streamflow measurements (Benettin et al., 2015b).

The RTD is conceptually different from the others, since it does not describe the travel time of the particles but the ages of all particles stored inside a catchment at a given time t (Botter et al., 2011). The age is then defined as $\tau_w = t(x) - t_{in}$, where $t(x)$ is the time of sampling at location x.
Because this reflects the inputs that occurred prior to t, it is actually a variation of a backward distribution (Benettin et al., 2015b). The RTD is useful for describing the catchment storage of water and pollutants (Botter et al., 2011). It furthermore constraints the ages sampled by the output fluxes, which determine the backward TTDs (Botter et al., 2011). Together the TTDs and RTDs contain information about the states and fluxes of all model components, thus enabling the description of the spatial complexity of a system while avoiding detailed descriptions of individual pathways to water and solutes (Benettin et al., 2015c).

3

Introduction of Frameworks

3.1. Introduction

Recognizing the shortcomings of standard conceptual models, the hydrological community has developed frameworks that are able to simulate the stream chemistry response while maintaining an holistic approach. The purpose of this study is to compare the performance of two of these frameworks. Both frameworks account for the advective transport processes of particles by including the effect of mixing in their conceptualization.

Starting point for each framework is the bucket model as introduced in paragraph 2.1.2. In order to include the stream chemistry response, both frameworks call for the inclusion of an additional storage volume, the passive storage. The passive storage represents the volume of water that is not hydrologically active, but partakes in the mixing process. As such, its name reflects its hydrological behaviour. The concept is supported by studies that have indicated that catchment storage is larger than the dynamic storage alone (Birkel et al., 2011; Vitvar et al., 2002).

Including a passive storage entails the introduction of a new calibration parameter that represents this hydrologically passive mixing volume. This parameter is then calibrated to hydrochemical data. In this manner the stream tracer response is calibrated to the total storage while the hydrological response is calibrated to only the active storage (the total storage minus the passive storage). The way each framework approaches the inclusion of a passive storage however is very different, as is clarified in the following paragraphs.

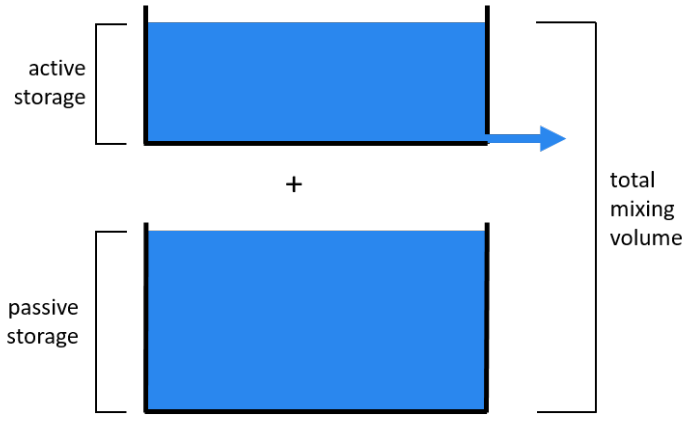

Figure 3.1: Addition of a passive storage

3.2. StorAge Selection functions

In paragraph 2.3, it was mentioned that the age distribution of water leaving a system is usually different than the age distribution of the water stored in the system, due to the effect of mixing. The StorAge Selection (SAS) approach is inspired by this concept. SAS functions are an expression of the ratio between the age distribution of the water leaving the system (a backward TTD), and the age distribution in the storage (RTD):

$$SAS = \frac{\overleftarrow{TTD}}{RTD} \tag{3.1}$$

SAS functions recapitulate the effect of hydrological processes that influence the age distributions of outflows (Rinaldo et al., 2015). As such, they can be used to impose mixing behaviour. How to interpret this conceptually is explained with help of Figure 3.2.

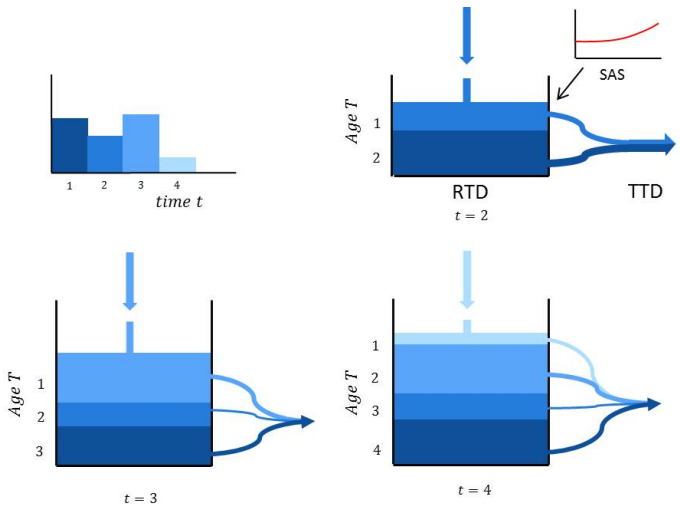

Figure 3.2: Mixing by application of a StorAge Selection function

At each time step, new water enters the system with age T=0. It is assumed that this water doesn't mix with other resident water while residing in the system. This way, a distribution of water with different ages is obtained (the RTD), where each layer of water still has its initial tracer concentration. From this RTD, a collection of volumes with different ages is sampled. The amount of water that's sampled from each layer is determined by the StorAge Selection function (SAS function), by imposing the ratio between the RTD and the distribution of ages in the flux (TTD). Only when the water leaves the bucket, volumes with different ages will mix, resulting in a new average tracer concentration of the water in the outgoing flux. By variation of the SAS function, it is possible to incorporate different degrees of mixing.

Several definitions have been developed to describe the SAS function. Botter et al. (2011) was the first to introduce an analytic formulation of this ratio. In this paper, the 'Age Function' was introduced as the ratio between the flux age distribution (a backward TTD) and the storage age distribution (RTD).

$$\omega_Q(T,t) = \frac{\overleftarrow{p}_Q(T,t)}{p_S(T,t)} \tag{3.2}$$

Where $\omega_Q(T,t)$ is the age function, representing ratio between the distributions of travel times T in the flux ($\overleftarrow{p}_Q(T,t)$) and the storage ($p_S(T,t)$), changing for every timestep t.

In figure 3.3, several variations of this Age Function are illustrated. Figure 3.3(a) represents uniform sampling, with a constant ratio of 1. In this scenario, the flux age distribution will be equal to the storage age distribution. In figure 3.3(b), the function expresses a preference for younger ages. This entails that the flux will sample water from the storage with a preference for younger ages, thus the water in the flux will relatively have more younger ages than the storage. Finally, figure 3.3(c) represents an Age function with a preference for older ages.

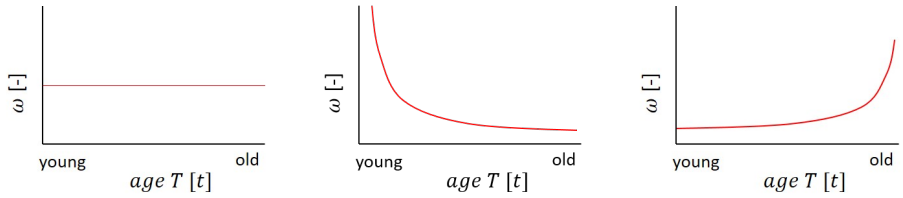

(a) uniform mixing (b) preference for young ages (c) preference for old ages

Figure 3.3: Variations of age functions

As illustrated in figure 3.5, the flux age distribution is generated by imposing the SAS function to the storage age distribution, according to the following equation:

$$\overleftarrow{p}_Q(T,t) = \omega_Q(T,t)\,p_S(T,t) \tag{3.3}$$

At every time step, there is a true SAS function. This is however impossible to measure directly unless every possible age in the transport volume is tagged (Rinaldo et al., 2015). Finding the right Age Function to represent the mixing behaviour of a catchment remains to be a challenge. A difficulty that is encountered when trying to find a characteristic Age Function, can be seen by taking the integral over equation 3.3:

$$1 = \int_0^\infty \omega_Q(T,t)\,p_S(T,t)\,dT \tag{3.4}$$

The Age Function must always satisfy this requirement to conserve probability (Harman, 2015). Because of the temporal variability of the age distributions however, the value of $\omega_Q(T,t)$ cannot be specified independently of the value of p_S. This makes it nearly impossible to parameterize $\omega_Q(T,t)$ in a closed form (Harman, 2015). To overcome this, Van der Velde proposed an alternative formulation.

3.2.1. Storage Outflow Probability (STOP) functions

Where Botter's Age function describes the ratio between the age distributions, STOP functions as proposed by Van Der Velde et al. (2012) describe the *probability* at time t of a stored water parcel to become discharge, evaporation or transpiration at time t, relative to the average probability of all particles to become discharge, evaporation or transpiration. This is achieved by a Smirnov transformation of travel time T:

$$g(T,t) \equiv \int_0^T p_S(\tau,t)\,d\tau \tag{3.5}$$

in which $g(T,t)$ is the cumulative probability of the resident time distribution for travel time T (Van Der Velde et al., 2012). Being a cumulative distribution function, $g(T,t)$ has a value between 0 and 1, where 0 corresponds to the youngest water in the storage and 1 to the oldest (see figure 3.4). As a result, the STOP functions can be defined as a function of g instead of T:

$$\omega_Q(g,t) = \frac{\overleftarrow{p}_Q(T(g,t),t)}{p_S(T(g,t),t)} \tag{3.6}$$

with $T(g,t)$ being the travel time corresponding to a certain value of g.

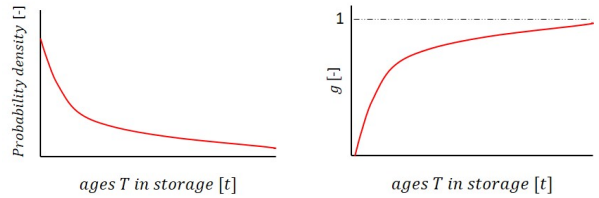

(a) storage residence time distribution

(b) cumulative

Figure 3.4: transformation into g(T,t)

This transformation has several advantages. Firstly, with equation 5.4, equation 5.3 can now be transformed to:

$$\overleftarrow{p}_Q(T(g,t),t) = \omega_Q(g,t)p_S(T(g,t),t) \tag{3.7}$$

$$1 = \int_0^1 \omega_Q(g,t)dg \tag{3.8}$$

The SAS function $\omega_Q(g,t)$ can now be identified with a probability distribution function (pdf) of a random variable on the interval [0,1] (Harman, 2015). Another advantage is that STOP functions are more constant in time than Age functions. For example, in case of a dry period all the water in the catchment would continue to age while the water would remain in roughly the same position. The cumulative probability of resident times however would be unchanged. Lastly, it is argued by Van Der Velde et al. (2012) that STOP functions have a clearer physical meaning than age functions, because they allow for the comparison of catchment mixing behaviour independent of their absolute travel time.

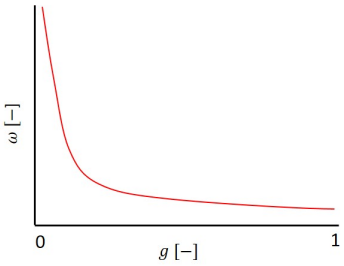

Figure 3.5: The STOP function, with a domain of [0,1], integrates to one and as such can be parameterized using existing PDFs.

3.3. Mixing coefficient

The second method to conceptualize mixing is the Mixing Coefficient approach (MC approach). For this framework, mixing is imposed by means of a dimensionless mixing coefficient C_M. This coefficient defines the amount of water that experiences exchange with resident water (water in the passive storage). It has a value between 0 and 1, with a mixing coefficient of 0 translating to no mixing at all and a mixing coefficient of 1 indicating complete mixing (Note that for this framework, it is not possible to apply a preference for older ages). This mixing coefficient can be chosen to be static or dynamic. For example, previous research has shown an influence of the soil moisture content on mixing dynamics (Hrachowitz et al., 2013). In these cases, it would be suitable to make the mixing coefficient dependent on the soil moisture conditions.

In the conceptualization in this research, the mixing is considered as instantaneous partial mixing between the active storage (S_a) and the passive storage (S_p), where only a part of the mobile water is mixed with the passive storage according to:

$$\frac{d(c_{a,i}S_{a,i})}{dt} = \sum_j (c_{I,j}I_{aFlux,j} + c_{p,i}(I_{pFlux,j} + I_{pS_{a,i}})) - \sum_k c_{a,i}O_k \tag{3.9}$$

$$\frac{d(c_{p,i}S_{p,i})}{dt} = \sum_j (c_{I,j}I_{pFux,j} + c_{a,j}I_{pS_{a,i}} - c_{p,i}(I_{pFlux,j} + I_{pS_{a,i}})) \tag{3.10}$$

where $I_{aFlux,j} = I_j(1 - C_{M,i}dt)$ and $I_{pFlux,j} = I_j C_{M,i}dt$ are the j individual water fluxes into the i active ($S_{a,i}$) and passive ($S_{p,i}$) storage compartments. $I_{pS_{a,i}} = C_{M,i}S_{a,i}$ represents the part of the active storage that mixes with the passive storage. Note that the water balance of the passive storage is zero, hence the same volume of water that enters the passive storage with the tracer concentration of the active storage (c_a) and the tracer concentration of the incoming flux (c_I) will leave the passive storage with tracer concentration of the passive storage (c_p).

In Figure 3.6, it is illustrated how this method can be interpreted. It can be seen how the traditional buckетmodel is expanded with an additional storage volume that accounts for the passive storage. When a flux enters the system, it will mix with the water in the active storage. Depending on the mixing coefficient, a part of this active storage will then mix with the water in the passive storage (see figure 3.6(b)) After mixing, the same volume of water will return to the active storage, resulting in new active storage concentration (c_a). From this (completely mixed) active storage, the discharge will leave the system.

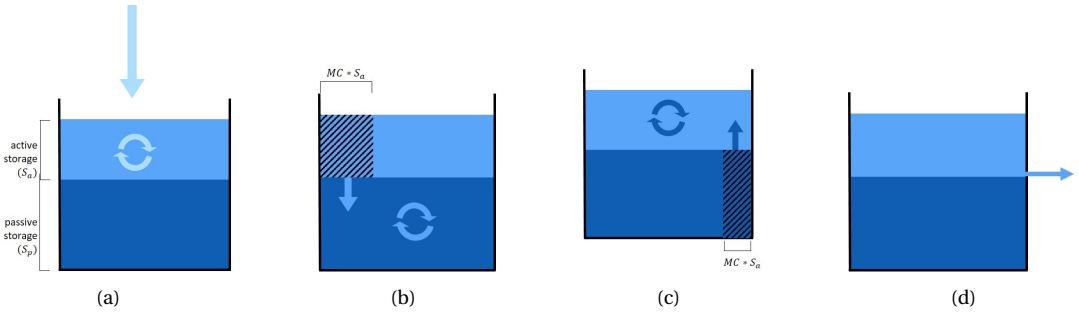

Figure 3.6: Mixing by application of a mixing coefficient

The above mentioned relations are slightly different than the method suggested in Hrachowitz et al. (2013), where only part of the incoming flux mixes with the passive storage, excluding the rest of the active storage from mixing. For this research, both approaches were considered. Because of a better performance (see Appendix A), the method where the active storage participates in the mixing process was chosen. It can also be argued that this method makes more sense conceptually, since it is probable that the amount of water that mixes is dependent on the volumes present in the subsurface and not necessarily on the rainfall at a specific moment in time.

From figure 3.6, it is easy to find a relation between the passive storage and the groundwater in the catchment that lies below the stream water level. One must however remain aware of the fact that although it is an attractive conceptualization, it may very well be that the hydrologically passive storage volume does not consist solely of the water below the stream water level. The passive storage can for example also indicate the volume of soil moister below field capacity. In that regard, one might as well depict the bucket as is done in Figure 3.7(c) and 3.4(d).

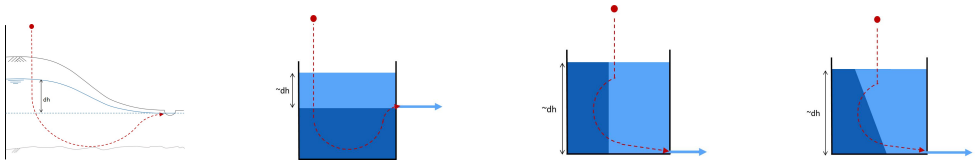

(a) (b) (c) (d)

Figure 3.7: Possible interpretations of the concept

4

Methodology

4.1. Introduction

To analyse the differences and similarities between the two frameworks, a comparative study is performed. For this, two hydrological models have been developed, one for each framework. The only variation between the two models is the choice of mixing assumptions.

4.2. Study area

The geographical setting of the two hydrological models lays in the Scottish Highlands. The catchment is located at elevations between 330 and 1020 m and experiences a sub-arctic climate with a mean annual temperature of 5.3° C. With 1100 mm yr-1, the mean annual precipitation is relatively low, whereby a significant amount of around 30% occurs as snow (Helliwell et al., 1998) The subsoil consists of fractured granite of lower Old Red Sandstone age and is covered by a 10 m thick layer of locally-derived drift deposit. The valley bottoms are covered by deep peats and follow are characterized by gentle slopes. On the other hand, steep slopes show freely draining alpine soils and podzols, leading to groundwater recharge and relatively high base flow levels (Soulsby et al., 2000). Alpine heath is the main land cover above 500 m, whereas at lower elevations, natural forests dominate the landscape (Pinus sylvestris, Betulaspp.; 10 %).

4.3. Data

The used data was analyzed over the period 1985-2006. Daily stream flow data were taken from the Scottish Environmental Protection Agency (SEPA). Daily precipitation was spatially interpolated from daily data available for adjacent sites of the British Atmospheric Data Centre (BADC, stations Dunstaffnage, Aberfoyle and Aviemore). Rainfall volumes were sampled on a weekly basis in open funnel bulk deposition samplers in the catchment. At the BADC stations Lagganalia, Cairngorm lift and Cairngorm summit, daily temperature data were available. By using the Penman-Monteith method, the potential evaporation was estimated and showed rough consistency with long-term estimates for the individual regions (1961-1990, MORECS).

The tracer used for this study was the chloride concentration. The chloride (Cl^-) concentration was analyzed at the individual catchment outlets from weekly or fortnighty sampled precipitation and simultaneous stream water dip samples. The samples were filtered through a 0.45 μm polycarbonate membrane filter subsequently analyzed by ion chromatography (Dionex DX100/DX120), determining the (Cl^-) concentrations. The bulk (Cl^-) concentrations of the preceding sampling period was weighted with the precipitation data and used to estimate the daily (Cl^-) input fluxes.

4.4. Hydrological model

Conceptual models consist of a combination of storage components that are linked through fluxes and can be customized based on perceived dominant processes. These storage components can be regarded as the building blocks of a conceptual model. To improve the stream chemistry response, one could rearrange the building blocks and its in- and outgoing fluxes to a situation that is deemed more realistic. Another way is to

improve the building blocks themselves. In this research, the emphasis is on the latter. It is therefore chosen to base the model structure on the model of the same catchment presented in the paper by Hrachowitz et al. (2013), and further research into an optimal model structure has (thus far) been left out of scope.

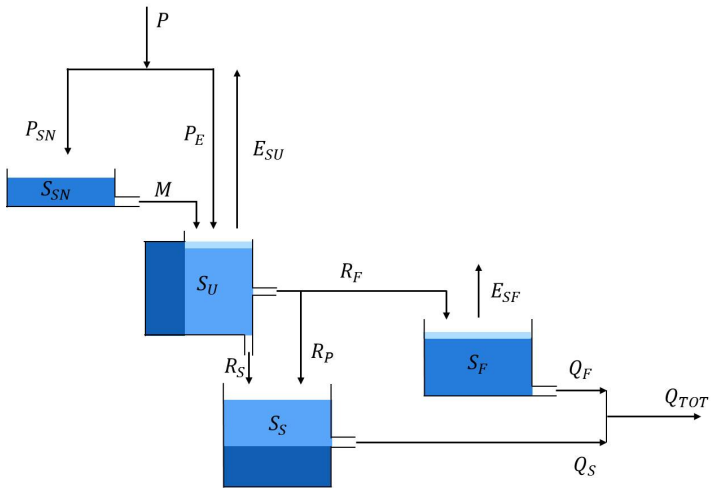

Figure 4.1: The hydrological model. Complete mixing occurs in S_{SN} and S_{SF}. Partial mixing, determined by either the SAS function or the mixing coefficient, occurs in S_U and S_S, where the dark blue shades indicate the passive storage and the medium blue shades indicate the active storage. The lighter blue shades on the upper layer of S_U and S_F represent the water that is used for evaporation and transpiration, since these processes do not include the uptake of the conservative tracer Cl^-.

The model is based on the model of Hrachowitz et al. (2013) and is structured in four different reservoirs: an unsaturated (S_U), a fast responding S_F, a slow responding S_S and an semi-distributed snow component (S_{SN}). For each elevation zone i the snow melt (M) was computed with the degree-day method, using the free calibration parameters threshold temperature (T_T) and melt factor (F_M).

The effective precipitation P_E is divided when reaching the soil. The water either infiltrates into the unsaturated zone (R_U) or runs off as excess water according to a runoff generation coefficient (C_R). Here C_R is a logistic function describing the soil moisture capacity in the root zone (S_{Umax}). The soil moisture content at field capacity and a shape factor (β) are thereby roughly reflected. Excess water is not stored in S_U. It either flows to S_F (R_F) or via preferential discharge to S_S (R_P), which depends on the coefficient (C_P). Water percolates from S_U to S_S. Subsequently, recharge of the slow responding reservoir (R_S) is represented by a linear relationship between the relative soil moisture and the maximum percolation capacity (P_{max}).

It is assumed that plants not only take up water from S_U (E_{SU}). They also tap water from S_F (E_{SF}), which was presumed to be within the root zone. Thus, the fraction for transpiration coming from S_U was described as linear function of the moisture content in S_U over the total moisture content in S_U and S_F. For the unsaturated zone (E_{SU}), transpiration was represented by a linear function of the relative soil moisture and threshold value L_P. The latter expresses the fraction of S_{Umax} below which the potential evaporation/transpiration E_P is limited by water available in S_U. Then again, E_{SF} was assumed to occur at potential rate as S_F represents a bundle of fast flow paths, which only activated under locally and temporally saturated conditions. Both S_F and S_S were conceptualized as linear reservoirs, wherefore water drainage (Q_{SF},Q_{SS}) is determined by the storage coefficients K_F and K_S.

Process	Water balance	Constitutive relationship
Snow	$\frac{dS_{SN}}{dt} = \sum_i P_{SN,i} - M_i$	$M = \sum_i min(S_{SN,i} F_M (T_i - T_T))$
Unsaturated zone	$\frac{dS_U}{dt} = P_E - E_{SU} - R_F - R_P - R_S$	$P_E = P_{TF} + M$
		$E_{SU} = E_P min(1, \frac{S_U}{S_{Umax}} \frac{1}{L_P}) C_P$
		$C_E = \frac{S_U}{S_U + S_F}$
		$R_U = (1 - C_R) P_E$
		$C_R (1 - CP) P_E$
		$R_P = C_R C_P P_E$
		$R_S = P_{max} (\frac{S_U}{S_{Umax}})$
		$C_R = \frac{1}{(1 + exp(\frac{-S_U / S_{Umax} + 0.5}{\beta})}$
Fast reservoir	$\frac{dS_F}{dt} = R_F - E_{SF} - Q_F$	$E_{SF} = min(E_P (1 - C_E), S_F)$
		$Q_F = K_F S_F$
Slow reservoir	$\frac{dS_S}{dt} = R_S + R_P - Q_S$	$Q_S = K_S S_S$

Table 4.1: State and flux equations of the models used in the analysis

4.5. Model calibration

Both models were calibrated to 5 years of data using Monte-Carlo sampling. The initial ranges were based on the results of previous research for the same catchment (Hrachowitz et al., 2013), and are presented in Table 4.2. In order to assess their performance, both models have been calibrated to the situation of complete mixing using 5000 Monte Carlo simulations. They have been calibrated to the Nash-Sutcliffe efficiency for the flows and to the Nash-Sutcliffe efficiency for the stream tracer concentration. The solution with the minimum Euclidean distance ($D_E = \sqrt{(1 - E_{NS,Q})^2 + (1 - E_{NS,C})^2}$) was chosen to continue the rest of the simulations with. Lastly, the value of K_S has not been calibrated in this research. Instead it was kept the same as earlier research that performed a MRC and set this parameter to 0.05.

It was not the purpose of this study to obtain the best model, it was the purpose to compare the results. To this end, this was found sufficient, and the best performing set has been chosen to continue the rest of the simulations with, for both models. These parameters are also presented in Table 4.2.

4.6. Calcution of tracer concentration

The calculation of the tracer concentration is different for each framework. In the MC approach, the tracer concentration is derived from the relations as expressed in paragraph 3.3. This entails that for every timestep, the tracer concentration of each bucket is calculated using the mass balance of that specific bucket. For the buckets with passive storage both the active storage concentration and the passive storage concentration are derived. The evolution of tracer concentration is then controlled by the input precipitation depth and tracer concentration, and the flux concentrations describing the tracer movement between storages.

For the SAS approach, a different calculation strategy is used. Here, the tracer concentrations of both the storages and the fluxes for each time step are calculated using convolution of the time distributions with the corresponding input tracer concentrations (McMillan et al., 2012). These time distributions are obtained through the application of flux tracking.

4.7. Flux tracking

For both frameworks, the transit time distributions are generated by tracking the in- and outfluxes of the system. To do this, the fluxes and states of all model components were represented in multidimensional

Parameter	Unit	Initial range	Calibrated parameter
T_T	(°C)	$-1.0-1.0$	0.65
F_M	$mm°C^{-1}d^{-1}$	$2-6$	4.08
$S_{U_{MAX}}$	(mm)	200-1200	276.55
β	$(-)$	$0-1$	0.3022
L_P	$(-)$	0-1	0.4937
K_F	(d^{-1})	0-3	0.5148
P_{MAX}	(mmd^{-1})	0-3	2.1932
C_P	$(-)$	0-1	0.5095
$S_{P,SS}$	(mm)	0-25000	17627
$S_{P,SU}$	(mm)	0-1000	250

Table 4.2: Parameters

matrices. Each matrix element represents a transport volume with a certain age. The time distributions can then be derived using the following equations:

$$p_S(T,t) = \frac{s(T,t)}{S(t)} \tag{4.1}$$

$$\overleftarrow{p}_Q(T,t) = \frac{q(T,t)}{Q(t)} \tag{4.2}$$

where $s(T,t)$ is the storage with travel time at T time t, $S(t)$ is the total storage of water inside the catchment, $q(T,t)$ is the discharge with travel time T at time t and $Q(t)$ is the total discharge at time t. Note that equation 5.2 is similar for all outgoing fluxes.

In figure 4.2, this is illustrated in a simplified manner. At each time step, a certain volume of water enters the system in the form of precipitation. The volume of water is represented in a matrix, as well as the water age T. From this, the RTD can be derived for each time step according to equation 5.1. The flux that leaves the system also has a certain age distribution, which can be calculated according to equation 5.2.

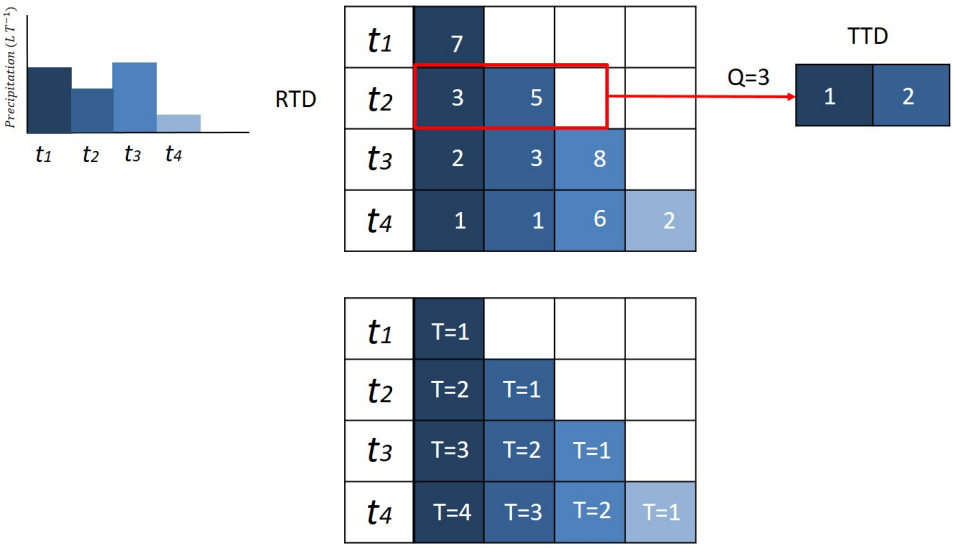

Figure 4.2: Flux tracking. Each timestep, the water that enters the system is represented in a multidimensional matrix.

4.8. Comparison of frameworks

The differences between the frameworks are compared by analysing the effect of each framework on the modeled behaviour. To make a sound comparison, it is necessary to apply the SAS function that corresponds to a particular mixing coefficient. For example, the situation of complete mixing is simulated by applying a uniform beta distribution in the SAS approach, which corresponds to a mixing coefficient of 1. The comparison becomes more complex when simulating a preference for younger or older water.

In previous literature by Hrachowitz et al. (2016), the relation between the two frameworks was depicted as in figure 4.3. It was suggested that e.g., a mixing coefficient of 0.2 would indicate that 20% of an incoming flux would be stored and mix with the resident water, while 80% of the incoming water would bypass the storage and be released without further interaction with resident water. A few comments can be made on this figure.

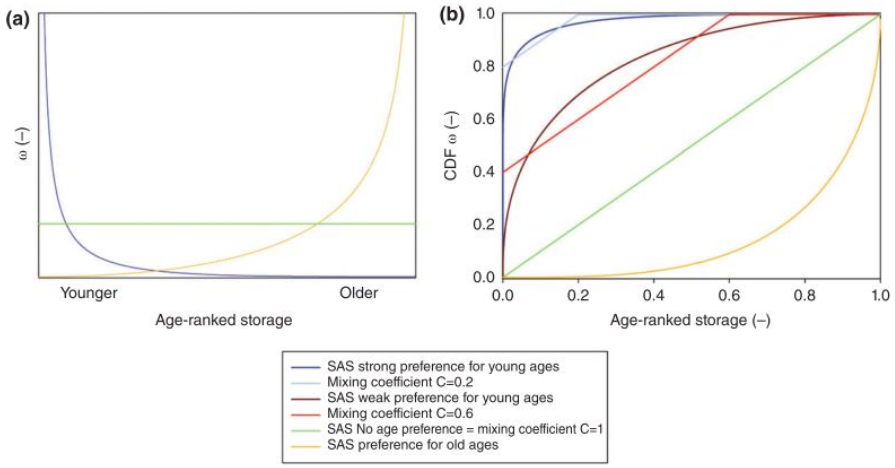

Figure 4.3: (a) Examples for SAS functions and (b) the comparison of cumulative SAS functions with the functionality of using the concept of the mixing coefficient(Hrachowitz et al., 2016)

Firstly, it should be noted that the Age functions as defined by Botter do not necessarily integrate to 1 (Van Der Velde et al., 2012; Harman, 2015). The SAS functions in figure 4.3 is therefore more likely to represent the relation between the STOP function and the cumulative RTD g, as presented in paragraph 3.2.1. Another observation that can be made is that in the MC framework, the fraction of the water that is mixed should mix with all ages that are available in the storage (there is complete mixing in the passive storage, see Figure 3.6). The cumulative SAS functions that are inferred from the MC approach, should therefore also converge to 1, as is illustrated in figure 4.4.

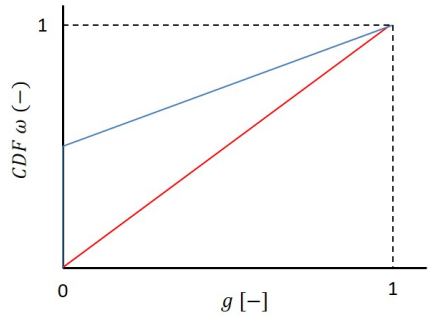

Figure 4.4: possible STOP functions inferred from the MC approach

The relation between the two frameworks however is even more complex. To investigate this, it is needed to take a closer look at the two concepts. As is illustrated in Figure 4.5(a), the SAS function determines the relation between the RTD and the TTD. The mixing coefficient on the other hand, imposes the mixing behaviour between the active and passive storage. This mixing behaviour then affects the relation between the RTD of the total storage and the TTD.

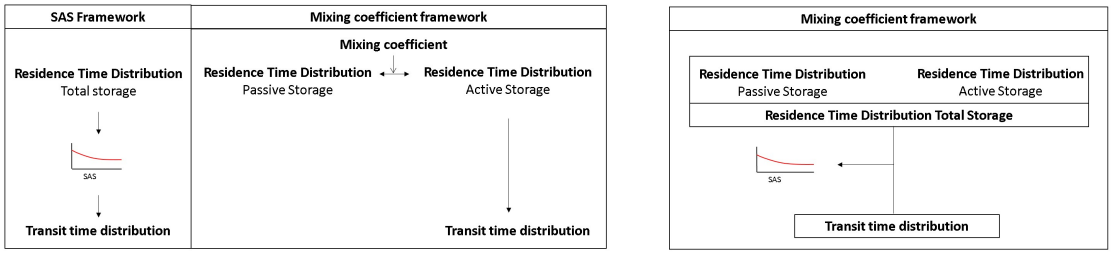

(a) (b)

Figure 4.5: obtaining the SAS function from the MC model results

It is possible to infer the corresponding SAS function from the results of the MC approach, as is illustrated in Figure 4.5(b). This function however does not only depend on the mixing coefficient, but also on the incoming and outgoing fluxes. This is clarified by having a closer look at the STOP functions as defined by Van der Velde:

$$\omega_Q(g,t) = \frac{\overleftarrow{p}_Q(T(g,t),t)}{p_S(T(g,t),t)} = \frac{q(T(g,t),t)}{s(T(g,t),t)} \frac{S(t)}{Q(t)} \tag{4.3}$$

By definition the STOP-function (or any type of SAS-function) at a specific time t depends on the fluxes and storages at that time. It would therefore only be possible to find a corresponding SAS-function for each mixing coefficient if the variability of the fluxes would be taken into account. This would entail a complex description of a mixing coefficient that depends on the time-variable hydrological conditions. For a more detailed description of the relation between the mixing coefficient and the SAS-function, the reader is referred to Appendix B.

It was however not the objective of this research to get both frameworks to be equal. On the contrary, the objective was to evaluate the different effects each method has on the modeled behaviour. In order to still be able to do this, the STOP-functions were inferred for each time-step from the results of the MC approach. A beta pdf was fitted to the average of these results. This beta pdf was then applied to the SAS-framework. The resulting pdfs are presented in chapter 5. The effect of the time variability on the relation between the two methods and the resulting beta pdf is also discussed in that chapter.

5

Results and discussion

5.1. Introduction

In this chapter the results will be presented and discussed. Firstly, the results of both frameworks with complete mixing are presented. Before applying partial mixing to both frameworks, corresponding STOP-functions to several mixing coefficients needed to be identified. The results of this process are presented in paragraph 5.3. Lastly, the effect of each framework on the system response is discussed for several cases of partial mixing.

5.2. Results complete mixing

According to expectation, in the case of complete mixing the two frameworks are functionally equivalent. In calibration, they performed equally well yielding similar results, as can be seen in 5.1. The results that are presented henceforth are all results of model simulations using the set of parameters as presented in section 4.5.

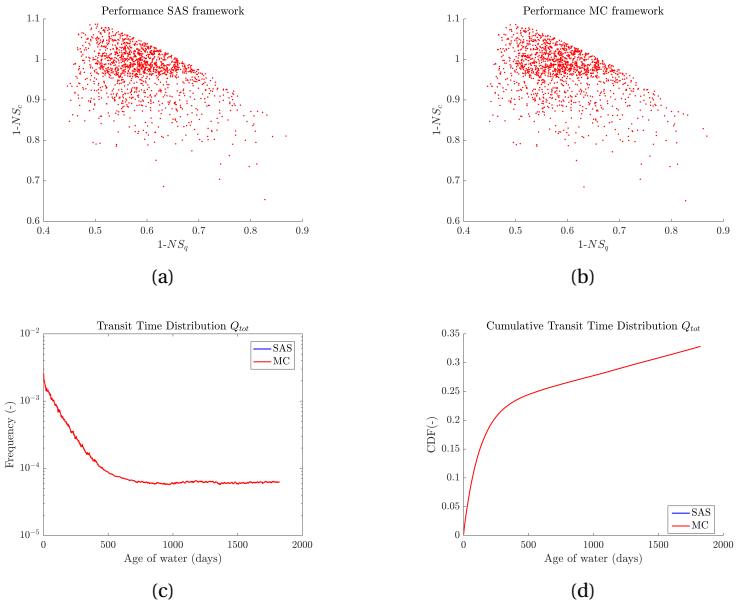

Figure 5.1: (a) and (b) present the Monte-Carlo simulation results. Optimal solutions are the ones closest to zero. (c) and (d) show the temporally averaged, flux-unweighted TTDs for the total discharge for both methods.

In Figure 5.1(c), the TTDs of the modeled discharge (Q_{TOT}) are presented. Both frameworks generated exactly the same values. Note that in Figure 5.1(d), the distribution does not add up to unity. This is because only

water younger than 5 years was tracked (see section 4.7). From Figure 5.1(d) it can be seen that 30% of the water in the discharge is younger than 5 years. This indicates that the catchment response has a great amount of water older than 5 years, which suggests that the effect of mixing is significant in this catchment.

5.3. Results selection STOP-function

For the situation of complete mixing, it is easy to find the STOP-function and Mixing Coefficient that are functionally equivalent. As presented in section 5.2, the values obtained with a Mixing Coefficient of 1 are identical to the values obtained with a uniform beta pdf as STOP-function.

When applying different degrees of mixing, it is more difficult to identify the relation between the STOP-function and the mixing coefficient. In paragraph 4.8, it was already stated that the original hypothesis about this relation as posed in previous research is likely to fall short due to the effect of time-variable fluxes. To confirm this, STOP-functions have been inferred from the model results of the MC approach. In Figure 5.2(a), several examples have been highlighted of specific times with varying values of unsaturated storage. It can be seen that as the volume of storage becomes higher, the preference for younger water increases. The graph in Figure 5.2(b) shows how the unsaturated storage changes over time. It can be observed that the storage in the unsaturated reservoir is highly variable.

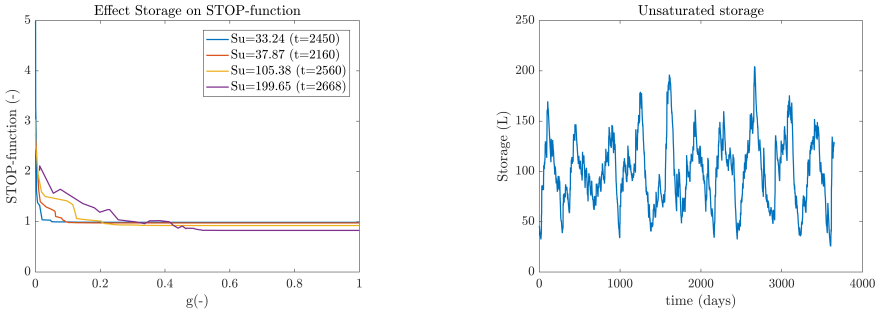

(a) (b)

Figure 5.2: The effect of storage on the STOP-functions that are inferred from the model results of the MC approach.

In Figure 5.3, all the graphs inferred daily from a model run period of 5 years are presented, for several mixing coefficients. The results show a large range of values, confirming the theory that SAS-functions resulting from the MC approach are time-dependent. In order to compare the effect of partial mixing behaviour on each framework, a beta pdf was fitted to the average of the results. Due to limitations that are explained in the next section, the SAS-functions (in this case STOP-functions) have only been inferred for the unsaturated storage.

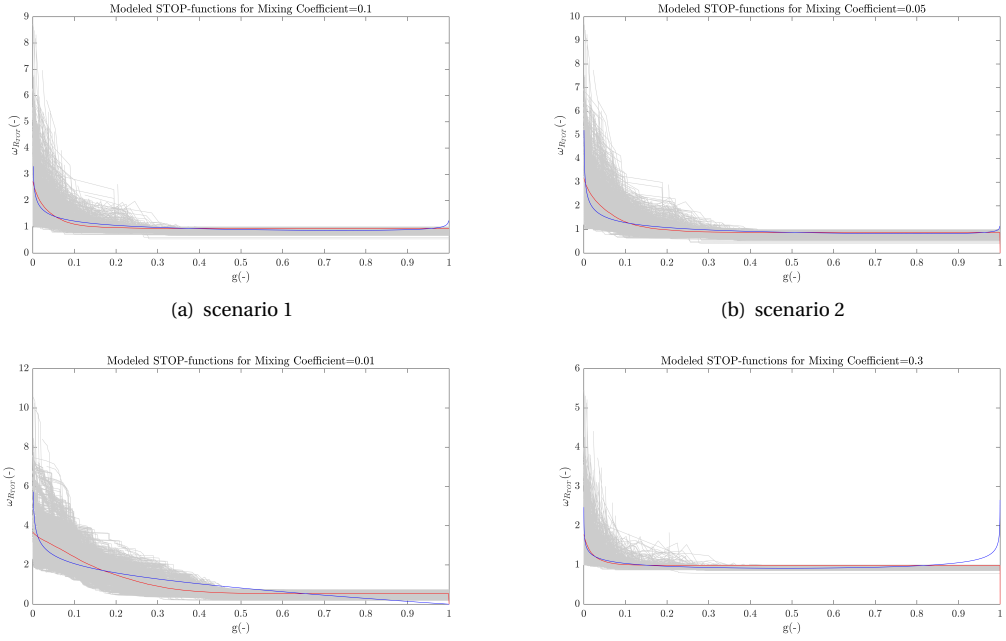

(a) scenario 1

(b) scenario 2

(c) scenario 3

(d) scenario 4

Figure 5.3: STOP-functions inferred from results MC approach. The red lines are the averaged values, the blue lines are the fitted beta pdfs

Scenario	Mixing Coefficient	α	β
1	0.1	0.7815	0.9240
2	0.05	0.7353	0.9343
3	0.01	0.9577	3.1432
4	0.3	0.8725	0.8647

Table 5.1: Resulting parameters of the beta distribution for each mixing coefficient

5.4. Results partial mixing

The results presented in Table 5.1 were applied to each model framework. Partial mixing has only been applied to the unsaturated storage. The initial strategy was to apply it to both the unsaturated and the slow storage. This was however found to be unfeasible. Before moving on to the final results, the reason for this is shortly explained.

5.4.1. Application of partial mixing to the slow storage reservoir

The passive storage of the slow storage is much larger than the passive storage of the unsaturated storage (see Table 4.2). As a result, the amount of water older than the period of measurement is also much higher. For clarification, the cumulative RTDs of both the unsaturated and slow storage are presented in Figure 5.4. It is clearly visible that while in the unsaturated storage almost all water is younger than 1000 days, in the slow storage approximately 20% is younger than 3650 days. This becomes a problem when applying the STOP-function.

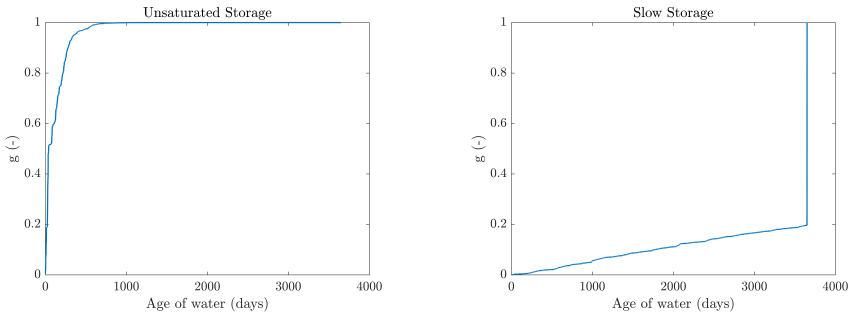

(a) (b)

Figure 5.4: Cumulative RTDs of unsaturated and slow storage
Obtained from the MC framework with a mixing coefficient of 0.05, at t=3650

As explained in paragraph 3.2.1, the STOP-function depends on the cumulative probability of the residence time distribution g. If only 20% of the water is tracked, the value for cumulative storage jumps from 0.2 to 1, as can be seen in 5.6(f). The value of the STOP-function derived for the oldest 80% of the water is then equal to the value of the STOP-function at g(T)=1 (see Figure 5.5(b)).

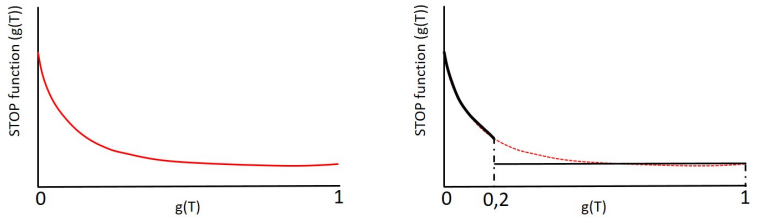

(a) (b)

Figure 5.5: Encountered difficulty when applying the SAS-framework with STOP-functions

As a result, the following condition that was presented in paragraph 3.2.1 does not hold:

$$1 = \int_0^1 \omega_Q(g,t)\,dg \tag{5.1}$$

If this condition is not fulfilled, the sum of the flux age distribution $\overleftarrow{p}_Q$ is not equal to 1, and the water balance is not met:

$$\overleftarrow{p}_Q(T(g,t),t) = \omega_Q(g,t)\,p_S(T(g,t),t) \tag{5.2}$$

Because it was not feasible to run the model for a time period long enough to avoid this effect (both due to the availability of data and the time needed to run the simulation), it was decided to only evaluate the effect of partial mixing for the unsaturated reservoir.

5.4.2. Application of partial mixing to the unsaturated storage reservoir

The results are presented for scenario 1, 2 and 3 as presented in Table 5.1. The beta pdf obtained for scenario 4 was discarded due to the high preference for older water, which can not be presented by the MC framework. Both the TTD of R_{tot} and of Q_{tot} are presented. R_{tot} is one of the fluxes leaving the unsaturated storage reservoir, and captures the effect of the mixing parameters on that specific bucket. The TTD of the total discharge Q_{tot} shows how this affects the total system response.

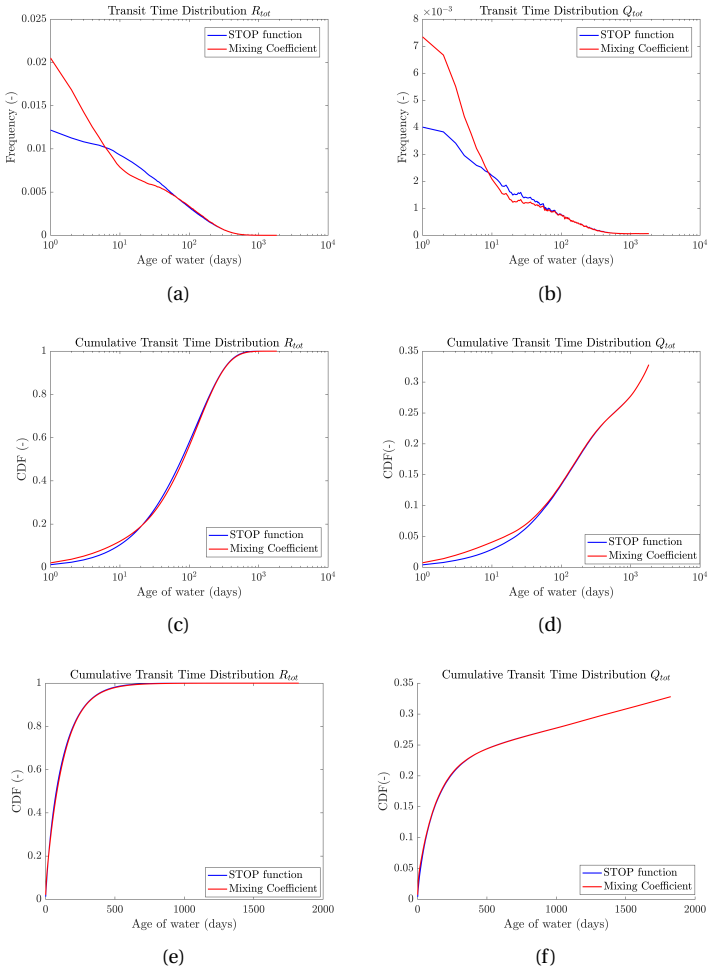

Figure 5.6: Results Mixing coefficient 0.1
All graphs show temporally averaged, flux-unweighted TTDs.
(a),(c) and (e) present the results for R_{TOT}.
(b),(d) and (f) present the results for Q_{TOT}

From Figure 5.6(e) and Figure 5.6(f), it follows that the differences between the two approaches are very small for this scenario. For the youngest water however, the relative difference is quite high. The effect of this difference in R_{TOT} (see figure 5.6(a)) is clearly visible in the total system response (figure 5.6(b)). As can be seen in Table 5.2, this does have an effect on the overall system performance. The effect however is very small. From Figure 5.6(d) it can be observed that the youngest water only contributes to less than 5% of the total flux.

Framework	D_E	$E_{NS,C}$	$E_{NS,Q}$
MC	0.97	0.20	0.45
SAS	0.92	0.26	0.45

Table 5.2: Performance mixing scenario 1

An important observation is that the results of the SAS approach and the MC approach, follow the same pattern as the differences between the fitted beta pdf and the average of the results presented in paragraph 5.3. This is also the case for mixing scenario 2. For this scenario, similar conclusions can be drawn as for mixing scenario 1. The ratio of young water is slightly higher than for scenario 1, due to the lowering of the mixing coefficient.

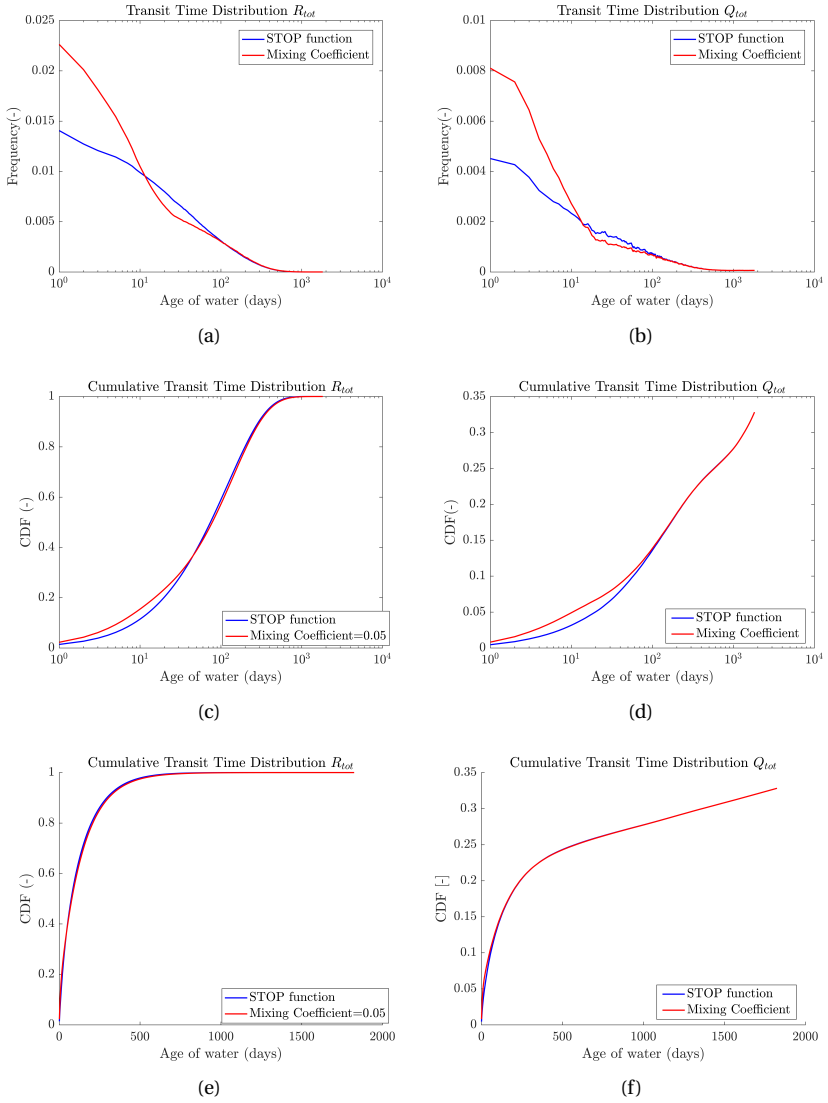

Figure 5.7: Results Mixing coefficient 0.05
All graphs show temporally averaged, flux-unweighted TTDs.
(a),(c) and (e) present the results for R_{TOT}.
(b),(d) and (f) present the results for Q_{TOT}

Framework	D_E	$E_{NS,C}$	$E_{NS,Q}$
MC	0.90	0.29	0.45
SAS	0.92	0.22	0.45

Table 5.3: Performance mixing scenario 2

On first sight, the results of scenario 3 seem different than for the other scenarios. The fraction of the youngest water in the fluxes is higher for the SAS approach. This while the pattern of the beta pdf in relation to the average of the MC model results is similar to that of scenario 1 and 2. When looking more closely however, the intersection between the beta pdf and the average of the results is at a slightly higher value of g(-). To see how this affects the results, it should be mentioned that the youngest water in the catchment does not correspond to a value of g=0. Note that g(T,t) is the cumulative probability of the RTD for travel time T. The lowest value of g(T,t) is therefore equal to the cumulative probability of the youngest water in the bucket at time t. For scenario 3, this value is generally lower than the value at intersection of the two lines, while for the other scenarios it is generally higher. Taking this effect into account, the results of this scenario also follow the patterns of the STOP-functions presented in figure 5.3.

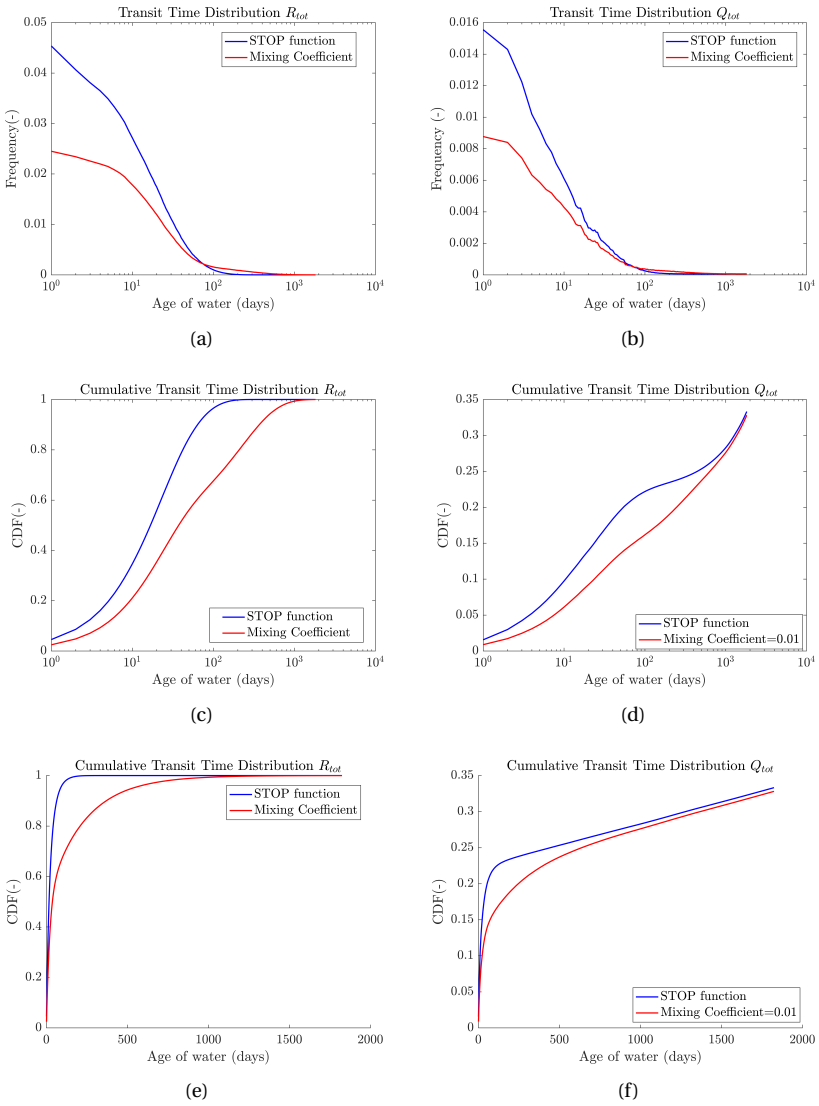

Figure 5.8: Results Mixing coefficient 0.01
All graphs show temporally averaged, flux-unweighted TTDs.

Framework	D_E	$E_{NS,C}$	$E_{NS,Q}$
MC	0.91	0.28	0.45
SAS	0.99	0.18	0.45

Table 5.4: Performance scenario 3

5.5. Synthesis

The time-variability of the relation between the Mixing Coefficient and the SAS-function brings to light an important conceptual difference between the two frameworks. The SAS approach imposes mixing behaviour through the relation of age distributions. It does so regardless of the hydrological conditions at that specific time. The mixing behaviour imposed by the MC approach on the other hand depends directly on the volumes of active and passive storage in the system. It therefore incorporates the effect of fluxes in and out the system. If the ratio of active and passive storage changes, the mixing behaviour changes as well. Generally, if the volume of active storage becomes higher, the effect of mixing becomes lower. This would translate to a higher preference for younger water. As such, this framework provides an attractive conceptualization of a situation where more water bypasses the storage as the soil moisture content gets higher. Several studies have found an effect of wetness conditions on TTDs. For example, McMillan et al. (2012) found a higher preference for younger water under wet conditions. Roa-García and Weiler (2010) on the other hand found that for events with higher antecedent wetness conditions there was less event water in the runoff. It therefore depends on the specific catchment whether the MC framework as defined in this research is suitable to capture these dynamics. In theory, the Mixing Coefficient could be made dependent on the storages, to counter the natural storage-dependency for cases where this is not suitable. In the same manner, the SAS function could be made dependent on the wetness conditions when this is needed. Both these measures would however increase the complexity of a model which is usually not desirable.

Another difference between the two frameworks is that unlike the MC framework, the SAS framework can impose a preference for older water. This might also be relevant for specific catchments. Van Der Velde et al. (2012) for example finds that for catchments where the bedrock slope dominates groundwater levels, there is a preferential discharge for relatively old water. However, both this effect and the effect of soil moisture conditions, could perhaps also be captured by activation and deactivation of hydrological processes in the system. This hypothesis is supported by previous research that found varying SAS functions for the overall system, as a result of multiple completely mixed buckets (e.g., Benettin et al., 2015a).

Finally, a difference that was not investigated in this research is the ability to account for different type of fluxes. In the SAS approach, it is relatively easy to apply a different type of SAS-function for different types of fluxes. In the MC approach, all the fluxes that leave a bucket select water with the same age distribution. Evaporation however is likely to extract water with a different age distribution than infiltration to the deeper groundwater layers. Furthermore, recent studies have indicated that water uptake by vegetation might also have a significant effect on mixing dynamics. Renée Brooks et al. (2010) identifies two water worlds, namely mobile water that reaches the stream and tightly bound water that is taken up by plants. These processes might be more easily approached with a framework that imposes behaviour to specific fluxes. It might also be possible to capture these dynamics by application of a separate transpiration bucket with a passive storage. Is however probable that the concept of two water worlds requires a different approach than either framework as presented in this research.

5.5.1. Limitations

It was already mentioned that the MC approach is unable to impose a preference for older ages. However, a great limitation of the SAS approach follows from the results in section 5.4.1. It was shown that for catchments with a large passive storage, complications arise in the application of the SAS-function. The model needs to run for a sufficient long time to overcome these complications. Even if enough data is available, this is computationally challenging due to the large matrices that are needed for these calculations.

6

Conclusions

The main objective of this research was to evaluate the differences and similarities between two frameworks that incorporate mixing in a catchment-scale conceptual model. These frameworks, the StorAge Selection and the Mixing Coefficient approach, have been applied to a hydrological model and their effects on the generated Transit Time Distribution have been evaluated.

In previous research it was suggested that the MC approach and the SAS approach are functionally equivalent (Hrachowitz et al., 2016). For the situation of complete mixing, the results of this research confirm this. As presented in section 5.2, the TTDs obtained with a Mixing Coefficient of 1 are identical to the TTDs obtained with a SAS-function. For partial mixing, the MC framework yields different results than the SAS framework. The results however imply that this difference is mainly caused by the differences between the average results of the MC approach and the beta pdf that was fitted to these averages, and was applied as SAS function.

In previous research by Hrachowitz et al. (2016), the hypothesis was also posed that for every SAS function there should be one mixing coefficient that approaches the same effect in the best way. Based on the result of this research this hypothesis is rejected. The results have demonstrated that the relation between the two approaches is variable throughout time. This is explained by a dependency on the hydrological fluxes in and out the system, as presented in paragraph 4.8.

Based on differences in their conceptualization, either framework might be more or less suitable for specific situations. For example, the MC approach already takes an effect of storage content into account. If the storage becomes higher, the effect of mixing becomes lower. Depending on the characteristics of a catchment, this might be an attractive conceptualization. The SAS framework however enables a preference for older water, which might also be better for specific catchments.

It is however likely that both frameworks are capable of replicating catchment-scale mixing behaviour, especially when applied in a conceptual model with multiple buckets representing different parts of the system. Based on this research, it can not be stated that one of the frameworks represents the behaviour of the system better. It can be concluded however that the MC approach is simpler in its conceptualization. It is found to be more transparent, and easier to implement in a model. Furthermore, it was shown that in cases with a large passive storage, the SAS approach needs a very long warm-up period in its simulation, which is not always feasible. Because of these reasons, it is recommended to continue research on optimization of the MC approach. The SAS framework however is a useful tool for model evaluation and catchment characterization.

There are still some interesting questions to be solved, which involve finding new ways to represent specific processes that influence mixing behaviour. This might be done by slightly altering the MC approach, or by rearranging the overall model structure. This is an interesting challenge for future research.

Appendices

A. Choice of mixing coefficient framework

In paragraph 3.3, it was mentioned that for the mixing coefficient method, two different frameworks were considered. Besides the framework that was discussed in the report, the approach as applied by Hrachowitz et al. (2013) was considered. In this approach, the following relation was used to define mixing:

$$\frac{d(c_{a,i}S_{a,i})}{dt} = \sum_j (c_{I,j}I_{a,j} + c_{p,i}I_{p,j}) - \sum_k c_{a,i}O_k \tag{6.1}$$

$$\frac{d(c_{p,i}S_{p,i})}{dt} = \sum_j (c_{I,j}I_{p,j} - c_{p,i}I_{p,j}) \tag{6.2}$$

where $I_{p,j} = I_j C_{M,i}dt$ and $I_{a,j} = I_j(1 - CM,idt)$ are the j individual water influxes to the i active and passive storage components. In figure 6.1 it is illustrated how to interpret this. When a flux enters the system, it will partially mix with the water in the passive storage. How much of the flux mixes is controlled by the mixing coefficient. The rest of the active storage does not participate in the mixing.

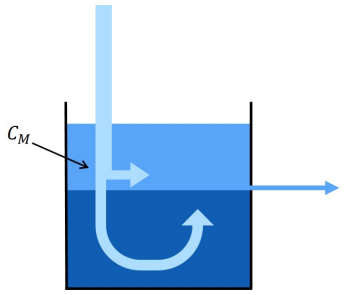

Figure 6.1: Mixing coefficient method when only the flux mixes

Both methods have been applied to the hydrological model as explained in chapter 4. From the calibration, the method where the active storage partakes in the mixing process led to better Nash-Sutcliffe efficiency values for the stream tracer concentrations (see figure 6.2).

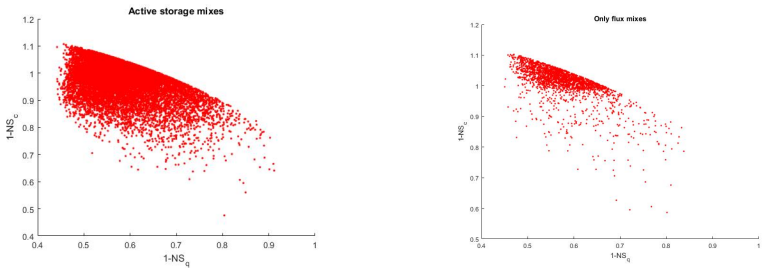

(a) active storage mixes (b) only flux mixes

Figure 6.2: 2D Pareto front for each method. For each method, 50000 Monte-Carlo samplings were performed

In figure 6.3 and 6.4, the effect of each method on the tracer concentrations in the passive and active storages is presented. It can be seen that the effect of a changing mixing coefficient is much more gradually when the active storage partakes in the mixing. The effects of a smaller mixing coefficient are very small in the unsaturated storage, which is because of a smaller passive storage volume that represents the limited mixing that occurs in this storage. In this storage, the patterns of the passive storage concentration are more closely related to the pattern of the active storage concentration. This is because it relies on the relation between the active and passive storage, rather than the relation between the flux and the passive storage. Conceptually, this seems more reasonable.

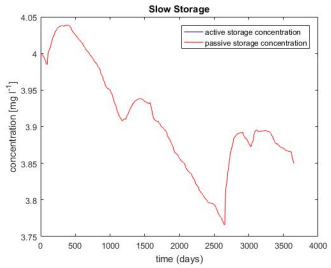

(a) active storage mixes $C_M = 1$

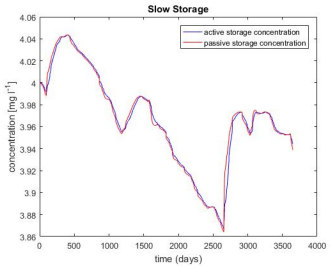

(b) only flux mixes $C_M = 1$

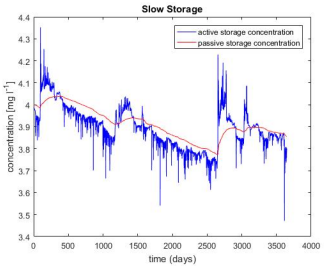

(c) active storage mixes $C_M = 0.5$

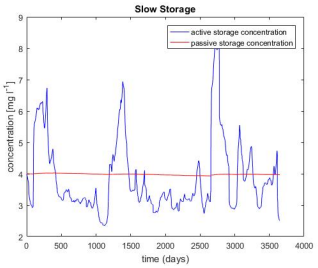

(d) only flux mixes $C_M = 0.5$

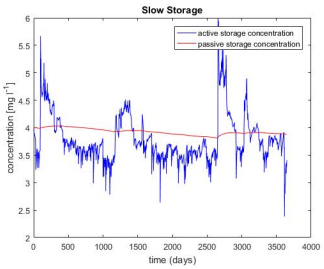

(e) active storage mixes $C_M = 0$.

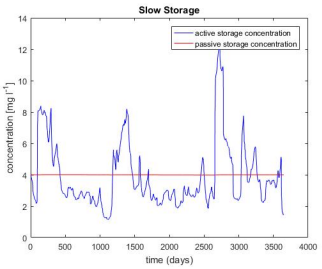

(f) only flux mixes $C_M = 0.1$

Figure 6.3: results Slow Storage

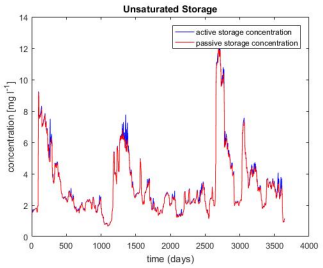

(a) active storage mixes $C_M = 1$

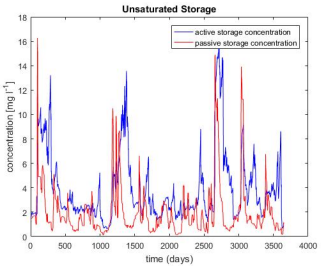

(b) only flux mixes $C_M = 1$

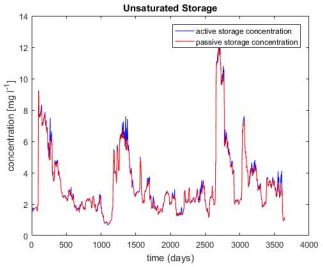

(c) active storage mixes $C_M = 0.5$

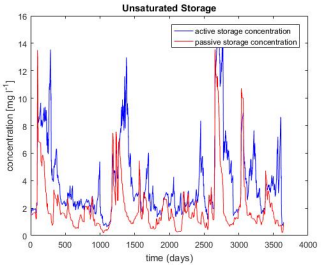

(d) only flux mixes $C_M = 0.5$

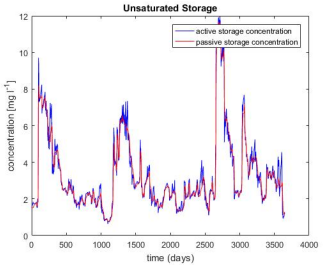

(e) active storage mixes $C_M = 0.1$

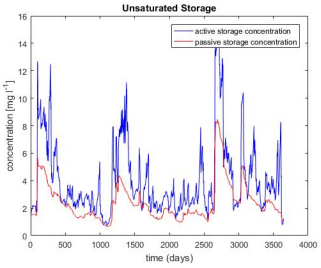

(f) only flux mixes $C_M = 0.1$

Figure 6.4: results Unsaturated Storage

B. The relation between TTD and RTD in the Mixing Coefficient framework

In section 4.8, it is mentioned that in the MC approach the relation between the TTD and the RTD (which can be expressed by a SAS function) depends on more than only the Mixing Coefficient. This is clarified by having a closer look at the processes that are depicted in Figure 6.5.

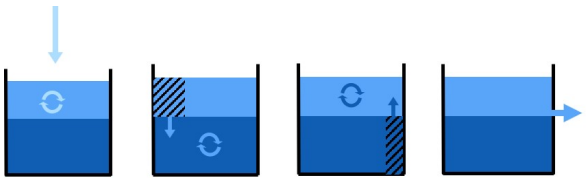

Figure 6.5

As summarized in figure 6.6, the SAS function can be defined as the ratio between the age distribution in the flux (TTD) and the age distribution in the storage (RTD). In the MC approach, the age distribution of the flux is equal to the age distribution of the active storage. As such, it is possible to rewrite the SAS function in terms of active and passive storage (see Figure 6.6):

$$SAS(T,t) = \frac{s_{act}(T,t)}{s_{act}(T,t) + s_{pas}(T,t)} * \frac{S_{active}(t) + S_{passive}}{S_{active}(t)} \tag{6.3}$$

where $s_{act}(T,t)$ is the active storage with travel time at T time t, $S_{active}(t)$ is the total volume of active storage, $s_{pas}(T,t)$ is the passive storage with travel time at T time t and $S_{passive}$ is the total volume of passive storage (which remains constant).Note that the concept is similar for the STOP-function as defined by Van der Velde, that is used in the rest of this research (section 3.2.1).

$$SAS(T,t) = \frac{Age\ distribution\ flux(T,t)}{Age\ distribution\ storage(T,t)}$$

$$Age\ distribution\ flux = \frac{q(T,t)}{Q(t)}$$

$$Age\ distribution\ storage = \frac{s(T,t)}{S(t)}$$

$$\Rightarrow \quad SAS(T,t) = \frac{q(T,t)}{s(T,t)} * \frac{S(t)}{Q(t)}$$

$$SAS(T,t) = \frac{q(T,t)}{s(T,t)} * \frac{S(t)}{Q(t)}$$

$$S(t) = S_{active}(t) + S_{passive}$$

$$s(T,t) = s_{act}(T,t) + s_{pas}(T,t)$$

$$\frac{q(T,t)}{Q(t)} = \frac{s_{act}(T,t)}{S_{active}(t)}$$

$$\Rightarrow \quad SAS(T,t) = \frac{s_{act}(T,t)}{s_{act}(T,t)+s_{pas}(T,t)} * \frac{S_{active}(t)+S_{passive}}{S_{active}(t)}$$

Figure 6.6

From this relation, it follows that the SAS function depends on the ratio between the volumes of active and passive storage. The Mixing Coefficient affects the ratio between the distributed values. The total amount of active storage however depends on the in- and outgoing fluxes. Thus, the relation between the TTD and RTD, inferred from the MC approach, is variable over time. As an example, the value of the Age function is derived

analytically for travel time $T = 1$, at a time t. The only water in the system with age 1 is the precipitation that fell in that time step, Prec(t).

Step by step:

1. Flux enters the active storage: $s_{act}(1,t) = 0 + Prec(t)$;
2. Part that stays in active storage: $s_{act}(1,t) = (1-MC) * s_{act}(1,t) = (1-MC) * Prec(t)$;
3. Part that enters passive storage:$s_{pas}(1,t) = 0 + MC * Prec(t)$;
4. Volume that moves from passive to active storage (of water with age T=1) = $(\frac{s_{pas}(1,t)}{S_{passive}+MC*S_{active}(t)}) * MC * S_{active}(t) = (\frac{MC*Prec(t)}{S_{passive}+MC*S_{active}(t)}) * MC * S_{active}(t)$;
5. new passive storage volume of water with age T=1 $s_{pas}(1,t) = MC * Prec(t)(1 - \frac{MC*S_{active}(t)}{S_{passive}+MC*S_{active}(t)})$;
6. new active storage volume of water with age T=1 $s_{act}(1,t) = (1-MC) * Prec(t) + (\frac{MC*Prec(t)}{S_{passive}+MC*S_{active}(t)}) * MC * S_{active}(t)$

with

$SAS(1,t) = \frac{s_{act}(1,t)}{s_{act}(1,t)+s_{pas}(1,t)} * \frac{S_{active}(t)+S_{passive}}{S_{active}(t)}$

this leads to

$SAS(1,t) = (1 - \frac{MC*S_{passive}}{MC*S_{active}(t)+S_{passive}}) * (\frac{S_{passive}+S_{active}(t)}{S_{active}(t)})$

which depends on the mixing coefficient, the storages and the fluxes.

References

Ali, M., Fiori, A., and Russo, D. (2014). A comparison of travel-time based catchment transport models, with application to numerical experiments. *Journal of Hydrology*, 511:605–618.

Benettin, P., Kirchner, J. W., Rinaldo, A., and Botter, G. (2015a). Modeling chloride transport using travel time distributions at Plynlimon, Wales.

Benettin, P., Kirchner, J. W., Rinaldo, A., and Botter, G. (2015b). Modeling chloride transport using travel time distributions at Plynlimon, Wales. *Water Resources Research*, pages 1–20.

Benettin, P., Rinaldo, A., and Botter, G. (2015c). Tracking residence times in hydrological systems: Forward and backward formulations. *Hydrological Processes*, 29(25):5203–5213.

Birkel, C., Soulsby, C., and Tetzlaff, D. (2011). Modelling catchment-scale water storage dynamics: Reconciling dynamic storage with tracer-inferred passive storage. *Hydrological Processes*, 25(25):3924–3936.

Botter, G. (2012). Catchment mixing processes and travel time distributions. *Water Resources Research*, 48(5):1–15.

Botter, G., Bertuzzo, E., and Rinaldo, A. (2011). Catchment residence and travel time distributions: The master equation. *Geophysical Research Letters*, 38(11):1–6.

Fenicia, F., Kavetski, D., Savenije, H., and Pfister, L. (2016). From spatially variable streamflow to distributed hydrological models: Analysis of key modeling decisions. pages 7548–7555.

Fenicia, F., McDonnell, J. J., and Savenije, H. H. G. (2008). Learning from model improvement: On the contribution of complementary data to process understanding. *Water Resources Research*, 44(6):1–13.

Fenicia, F., Wrede, S., Kavetski, D., Pfister, L., Hoffmann, L., Savenije, H. H. G., and McDonnell, J. J. (2010). Assessing the impact of mixing assumptions on the estimation of streamwater mean residence time. *Hydrological Processes*, 24(12):1730–1741.

Godsey, S. E., Aas, W., Clair, T. A., de Wit, H. A., Fernandez, I. J., Kahl, J. S., Malcolm, I. A., Neal, C., Neal, M., Nelson, S. J., Norton, S. A., Palucis, M. C., Skjelkv??le, B. L., Soulsby, C., Tetzlaff, D., and Kirchner, J. W. (2010). Generality of fractal 1/f scaling in catchment tracer time series, and its implications for catchment travel time distributions. *Hydrological Processes*, 24(12):1660–1671.

Harman, C. J. (2015). Time-variable transit time distributions and transport: Theory and application to storage-dependent transport of chloride in a watershed. *Water Resources Research*, 51(1).

Helliwell, R. C., Soulsby, C., Ferrier, R. C., Jenkins, A., and Harriman, R. (1998). Influence of snow on the hydrology and hydrochemistry of the Allt a' Mharcaidh, Cairngorm mountains, Scotland. *Science of the Total Environment*, 217(1-2):59–70.

Hrachowitz, M., Benettin, P., Fovet, O., Howden, N., Ruiz, L., and Wade, A. (2016). Transit times - the link between hydrology and water quality at the catchment scale. *WIREs Water*, in press.

Hrachowitz, M. and Clark, M. P. (2017). HESS Opinions: The complementary merits of competing modelling philosophies in hydrology. *Hydrology and Earth System Sciences*, 21(8):3953–3973.

Hrachowitz, M., Savenije, H., Bogaard, T. A., Tetzlaff, D., and Soulsby, C. (2013). What can flux tracking teach us about water age distribution patterns and their temporal dynamics? *Hydrology and Earth System Sciences*, 17(2):533–564.

Hrachowitz, M., Soulsby, C., Tetzlaff, D., Dawson, J. J. C., Dunn, S. M., and Malcolm, I. A. (2009a). Using long-term data sets to understand transit times in contrasting headwater catchments. *Journal of Hydrology*, 367(3-4):237–248.

Hrachowitz, M., Soulsby, C., Tetzlaff, D., Dawson, J. J. C., and Malcolm, I. A. (2009b). Regionalization of transit time estimates in montane catchments by integrating landscape controls. *Water Resources Research*.

Hrachowitz, M., Soulsby, C., Tetzlaff, D., Malcolm, I. A., and Schoups, G. (2010). Gamma distribution models for transit time estimation in catchments: Physical interpretation of parameters and implications for time-variant transit time assessment. *Water Resources Research*, 46(10).

Kirchner, J. W. (2006). Getting the right answers for the right reasons: Linking measurements, analyses, and models to advance the science of hydrology. *Water Resources Research*, 42(3):1–5.

Kirchner, J. W., Feng², X., and Neal#, C. (2000). Fractal stream chemistry and its implications for contaminant transport in catchments The time it takes for rainfall to travel through a catchment and reach the stream is a fundamental hydraulic parameter that controls the retention of soluble contaminant. *Nature*, 403.

McDonnell, J. J. (2014). The two water worlds hypothesis: ecohydrological separation of water between streams and trees? *Wiley Interdisciplinary Reviews: Water*, 1(4):323–329.

McDonnell, J. J., McGuire, K., Aggarwal, P., Beven, K. J., Biondi, D., Destouni, G., Dunn, S., James, A., Kirchner, J., Kraft, P., Lyon, S., Maloszewski, P., Newman, B., Pfister, L., Rinaldo, A., Rodhe, A., Sayama, T., Seibert, J., Solomon, K., Soulsby, C., Stewart, M., Tetzlaff, D., Tobin, C., Troch, P., Weiler, M., Western, A., Wörman, A., and Wrede, S. (2010). How old is streamwater? Open questions in catchment transit time conceptualization, modelling and analysis. *Hydrological Processes*, 24(12):1745–1754.

McGlynn, B., McDonnell, J., Stewart, M., and Seibert, J. (2003). On the relationships between catchment scale and streamwater mean residence time. *Hydrological Processes*.

McGuire, K. J. and McDonnell, J. J. (2006). A review and evaluation of catchment transit time modeling. *Journal of Hydrology*.

McGuire, K. J., McDonnell, J. J., Weiler, M., Kendall, C., McGlynn, B. L., Welker, J. M., and Seibert, J. (2005). The role of topography on catchment-scale water residence time. *Water Resources Research*, 41(5):1–14.

McMillan, H., Tetzlaff, D., Clark, M., and Soulsby, C. (2012). Do time-variable tracers aid the evaluation of hydrological model structure? A multimodel approach. *Water Resources Research*, 48(5).

Niemi, A. J. (1977). Residence time distributions of variable flow processes. *Int. J. Appl. Radiat. Isotopes*, 28(10-11):855–860.

Renée Brooks, J., Barnard, H. R., Coulombe, R., and McDonnell, J. J. (2010). Ecohydrologic separation of water between trees and streams in a Mediterranean climate. *Nature Geoscience*, 3(2):100–104.

Rinaldo, A., Benettin, P., Harman, C., Hrachowitz, M., McGuire, K., van der Velde, Y., Bertuzzo, E., and Botter, G. (2015). Water Resources Research. *Water Resources Research*, pages 4840–4847.

Roa-García, M. C. and Weiler, M. (2010). Integrated response and transit time distributions of watersheds by combining hydrograph separation and long-term transit time modeling. *Hydrology and Earth System Sciences*, 14(8):1537–1549.

Sivapalan, M. (2005). Pattern, Process and Function: Elements of a Unified Theory of Hydrology at the Catchment Scale. In *Encyclopedia of Hydrological Sciences*, number APRIL 2006, pages 193–219.

Soulsby, C., Malcolm, R., Helliwell, R., Ferrier, R. C., and Jenkins, A. (2000). Isotope hydrology of the Allt a' Mharcaidh catchment, Cairngorms, Scotland: Implications for hydrological pathways and residence times. *Hydrological Processes*, 14(4):747–762.

Soulsby, C., Tetzlaff, D., and Hrachowitz, M. (2009). Tracer and transit times: windows for viewing catchment scale storage? *Hydrological Processes*, 23:3503–3507.

Speed, M., Tetzlaff, D., Soulsby, C., Hrachowitz, M., and Waldron, S. (2010). Isotopic and geochemical tracers reveal similarities in transit times in contrasting mesoscale catchments. *Hydrological Processes*, 24(9):1211–1224.

Tetzlaff, D., Soulsby, C., Hrachowitz, M., and Speed, M. (2011). Relative influence of upland and lowland headwaters on the isotope hydrology and transit times of larger catchments. *Journal of Hydrology*, 400(3-4):438–447.

Van Der Velde, Y., De Rooij, G. H., Rozemeijer, J. C., Van Geer, F. C., and Broers, H. P. (2010). Nitrate response of a lowland catchment: On the relation between stream concentration and travel time distribution dynamics. *Water Resources Research*, 46(11):1–17.

Van Der Velde, Y., Torfs, P. J. J. F., Van Der Zee, S. E. A. T. M., and Uijlenhoet, R. (2012). Quantifying catchment-scale mixing and its effect on time-varying travel time distributions. *Water Resources Research*, 48(6):1–13.

Vitvar, T., Burns, D. A., Lawrence, G. B., McDonnell, J. J., and Wolock, D. M. (2002). Estimation of baseflow residence times in watersheds from the runoff hydrograph recession: method and application in the Neversink watershed, Catskill Mountains, New York. *Hydrological Processes*.

Wagener, T., Sivapalan, M., McDonnell, J., Hooper, R., Lakshmi, V., Liang, X., and Kumar, P. (2004). Predictions in ungauged basins as a catalyst for multidisciplinary hydrology. *Eos, Transactions American Geophysical Union*, 85(44):451.

Zuber, A. (1986). On the interpretation of trcer data in variable flow systems. *Journal of Hydrology*, 86:45–57.